

Effect of Parameter Change upon the Extra-tropical Atmospheric Variability

Hanneke E. Levine-Moolenaar^{1,2}, Frank M. Selten¹ and Johan Grasman^{2,3}

¹Royal Netherlands Meteorological Institute, De Bilt, The Netherlands

²Wageningen University, Wageningen, The Netherlands

³Corresponding author, address: Biometris, Wageningen University, Postal Box 100, 6700AC

Wageningen, The Netherlands; Email: johan.grasman@wur.nl.

May 5, 2009

Abstract

Climate models contain numerous parameters with uncertain values. In the context of climate prediction, it is relevant to obtain an estimate of the range of outcomes given the parameter uncertainty. Taking an ensemble of simulations with randomly perturbed parameters would require an extremely large sample, because most random perturbations do not have much impact. In this study we select parameter perturbations that potentially change the climate effectively. We consider a dry, spectral quasi-geostrophic, three-level model on the sphere (T21QGL3). Two approaches are considered. First, using the theory of empirical orthogonal functions (EOFs), parameter perturbations are explored that directly act in the direction of a preferred flow regime. Next the changing sensitivity to perturbations along the chaotic attractor of a circulation model is analyzed. Frequently short intervals of high sensitivity are passed. Using the adjoint method we select the first singular vector denoting the direction of the parameter perturbation having the largest effect in such an interval. For the first 1000 intervals with the highest sensitivity, this vector is taken for the

direction of the parameter perturbation of the system integrated over 100,000 days. As a measure of change we compute the probability density of the dominant patterns of variability, since these strongly impact regional climates. The parameter perturbations are limited to constant terms in the equations yielding a vector of 1449 values. The approach based on the adjoint method is the most successful: compared with random search the effect of the best perturbation in the sample is a factor 20 larger.

1. Introduction

Uncertainty in the outcome of climate models is widely recognized, see Fleming (1993), Allen (2003), Murphy et al. (2004), Stocker (2004), Stainforth et al. (2005) and IPCC (2001). A contributing factor is uncertainty in the model parameters. Most of the model parameters are not exactly known so an uncertainty analysis should be part of a study on the long term dynamics of the climate. Of special interest is the range of possible outcomes of the climate model, given the range of parameter uncertainties. A practical method to identify the parameter perturbations that yield the more extreme outcomes is lacking. We refer to these parameter perturbations as effective parameter perturbations. Fleming (1993) conducted a preliminary analysis on uncertain model parameters in the context of simple non-linear dynamical systems. He stated that there is a need to establish a scientific methodology for identifying and quantifying the impacts of uncertainty. For complex General Circulation Models (GCMs) he concluded that the Monte Carlo approach is the only practical solution to obtain uncertainty estimates despite the lack of rigor in the determination of the sample size and the enormous computational effort that is required. To provide a reliable estimate of the spread of possible regional climate changes, a large ensemble of climate predictions is needed, in which parameters are chosen such that the widest range of uncertainties is captured (Murphy et al., 2004). In a first attempt to evaluate climate sensitivity due to anthropogenic climate

change (assuming a doubled CO₂ concentration) they compiled an ensemble of 4×10^6 model versions of an atmospheric model coupled to a mixed-layer ocean, with randomly chosen multiple parameter perturbations. Stainforth et al. (2005) presented results from the 'climate.net' experiment in which climate simulations are performed on personal computers all around the world. A central server distributes the computation tasks through the internet and collects the results. The experiments show that impacts of different parameter perturbations do not combine linearly in the regional climate response, partially invalidating the Murphy et al. (2004) study.

If one is interested in the climate mean response to a small change in forcing, an alternative approach, based on the fluctuation-dissipation theorem (Leith, 1975), has been developed. This theorem states that by observing the natural fluctuation of a system with certain properties a linear operator can be constructed that gives the response of the system to an external stimulus of sufficiently weak amplitude. The most realistic test of the theorem's applicability to the atmosphere so far is described in Gritsun and Branstator (2007). This approach does not suffer from sampling issues and subjective expert judgements. However, it cannot assess the impact of parameters that occur in products with state variables in the governing equations and only evaluates the response of the mean state.

In this study we evaluate two directed search approaches to obtain parameter perturbations that potentially cause a large change in regional climates. Regional climates depend strongly on the frequency of occurrence of preferred atmospheric variability patterns, like for Europe the North Atlantic oscillation (Hurrell, 1995; Visbeck et al., 2001) or European blocking (Carril et al., 2008). As a measure of climate change we therefore evaluate the change in a probability density function (PDF) describing the presence of dominant circulation structures and not just the change in the mean state.

For our investigation we use a dry, spectral quasi-geostrophic, three-level model on the sphere (T21QGL3), see Marshall and Molteni (1993). First, employing the theory of empirical orthogonal functions (EOFs), we explore parameter perturbations that directly act in the direction

of a preferred flow regime. Since EOF1 is related to the most prominent preferred flow regime (North Atlantic oscillation), it is very well possible that an additional constant forcing of the system in the direction of EOF1 turns out to be an effective way to change the climate. We apply a perturbation to the constant forcing vector that is introduced to compensate the fact that the model potential vorticity tendencies do not vanish in the averaged equations. This perturbation is taken in the direction of EOF1 with a length of resp. 5 and 10% of the forcing vector. It indeed induces a change in the PDF measuring the distribution in time of the different regimes. Next the changing sensitivity to perturbations along the chaotic attractor of a global circulation model is taken as a clue to find a shift in the forcing parameter vector that most effectively changes the statistics of the flow in the long term. From time to time short intervals of high sensitivity are passed. Using the adjoint method we select the first singular vector denoting the direction of the parameter perturbation having the largest effect in such an interval (Errico, 1997). In order to analyze this effect upon the regional climate the perturbation is next applied to the full model over an extended time interval. Repeating the procedure for many short highly sensitive intervals at the attractor we can compare the different results and take the best of them. The method was developed in Moolenaar and Selten (2004) in the context of the three-component Lorenz model of Rayleigh-Benard convection (Lorenz, 1963). The T21QGL3 model produces a quite realistic simulation of the extra-tropical wintertime circulation (Corti et al., 1997). It has been used for adjoint sensitivity analysis with respect to uncertainty in both the initial conditions and the forcing (Oortwijn and Barkmeijer, 1995), see also Barkmeijer et al. (2003). In a way comparable to the Lorenz '63 model, the T21QGL3 model shows preferred circulation structures (Selten and Branstator, 2004). Whereas the Lorenz 63 model only has two “preferred flow regimes”, the T21QGL3 model contains several of them. Both models show sensitivity to initial conditions as well as sensitivity to the perturbation of parameters depending on the state of the model. Consequently, the dynamics of the T21QGL3 model bears sufficient similarities to the Lorenz 63 model to also apply the adjoint method for finding effective parameter perturbations to this system.

In Section 2 the T21QGL3 model is described and a measure of climate change is introduced. In Section 3 both the introduction of a perturbation in the direction of EOF1 and the use of the adjoint method for finding effective parameter perturbations are explained and applied to the T21QGL3 model. In order to judge the meaning of the results we obtained, we also carry out a random selection method in Section 4 and compare the outcomes in Section 5, where we also discuss the wider scope of the adjoint method.

2. Climate sensitivity analysis using empirical orthogonal functions

In the extratropics, the atmospheric circulation can be well approximated by quasi-geostrophic equations. These equations are filtered prognostic equations (gravity waves are absent) and can be written in terms of only one variable, the quasi-geostrophic potential vorticity. Here, the quasi-geostrophic (QG) T21-model is used, which is a spectral, 3-level model, as described by Marshall and Molteni (1993). For the potential vorticity a series expansion in spherical harmonics is made. The time dependent coefficients of this expansion are the state variables of the model. The series of spherical harmonics used in the representation of horizontal fields has a triangular truncation at total wavenumber 21 (T21). The model integrates prognostic equations for the QG potential vorticity at 200 hPa (level 1), 500 hPa (level 2) and 800 hPa (level 3),

$$\frac{\partial q_k}{\partial t} = -J(\psi_k, q_k) - D_k(\psi) + S_k \quad \text{with} \quad J(\psi_k, q_k) = \frac{\partial \psi_k}{\partial \lambda} \frac{\partial q_k}{\partial \mu} - \frac{\partial \psi_k}{\partial \mu} \frac{\partial q_k}{\partial \lambda}, \quad k = 1, 2, 3, \quad (1)$$

where q_k is the potential vorticity (PV) and ψ_k the streamfunction at level k , D_k is a linear operator that represents dissipation, S_k is an artificial forcing, J the Jacobian in which λ represents the longitude and μ the sine of the latitude. Eq.(1) represents a vertical discretization of the quasi-

geostrophic potential vorticity equation (Holton, 1992). Details on the derivation of (1) and on the relation between the vectors q and ψ can be found in Marshall and Molteni (1993). It is assumed that the multi-level PV is a linear function of the multi-level streamfunction vector ψ . At each level the PV has 483 spectral components, so that the model has in total 1449 degrees of freedom. Instead of expressing the state of the system in the amplitudes of the spectral components we use *Empirical Orthogonal Functions*, see Preisendorfer (1988). These EOFs form an orthonormal system $\{e^{(1)}, e^{(2)}, \dots\}$. The streamfunction vector $\psi(t)$ has a time mean $\overline{\psi(t)}$. The difference between the two is approximated by the projection upon the first p EOFs:

$$\psi(t) - \overline{\psi(t)} = \sum_{i=1}^p a_i(t) e^{(i)} \quad \text{with} \quad a_i(t) = \langle \psi(t) - \overline{\psi(t)}, e^{(i)} \rangle, \quad (2ab)$$

where $\langle \cdot, \cdot \rangle$ denotes the Euclidian innerproduct with norm $|\mathbf{v}| = \langle \mathbf{v}, \mathbf{v} \rangle^{1/2}$. In our case $p = 483$.

Under the assumption that the EOF amplitudes are uncorrelated in time the total variance in the streamfunction equals the sum of the eigenvalues μ_i of the matrix $A(t) = a(t) a(t)^T$:

$$\text{Var}\{\psi(t)\} = \sum_{i=1}^p \mu_i. \quad (3)$$

The eigenvalues corresponding to the EOFs fall off very quickly, see Figure 1. Given are the eigenvalues of the first 100 EOFs of the T21QGL3 model calculated from 100,000 daily fields of the 500 hPa streamfunction over the northern hemisphere. It is observed that most information about the variability is contained in the first leading EOFs. The first 10 EOFs contain 55% of the information about the variability. By projecting the data along these dominant EOFs and truncating the summation (2a) at a certain $n < p = 483$ we can reduce the dimension of the full EOF space considerably and still retain a good global view of the dynamical range of the system. A special

property of the EOFs is that for a given truncation n no other basis set can explain more of the average variance (Lorenz, 1956; North et al., 1982).

The leading EOFs are an indication for the presence of *preferred flow regimes*. In the T21QGL3 model EOF1 is strongly related to the North Atlantic Oscillation (NAO) and EOF2 may represent the Pacific North American pattern (PNA). The NAO is important for the regional climate in Western Europe. A stronger NAO results in fewer easterlies and more westerlies which cause milder winters in Western Europe (Hurrell, 1995). We will examine the effect of forcing parameter perturbations upon the occurrence of preferred flow regimes. An important question is formulated as follows: do parameter changes have a notable influence on the NAO and therefore on the climate in Western Europe? Analysis of the EOFs can give us information about the effect upon the climate. A climate is characterized by the statistical properties of the circulation over an extended time interval ($\sim 10^5$ days). In Figure 2 EOF1 - EOF4 of the T21QGL3 model are shown. The probability density functions (PDFs) of the first a_i 's, sampled over the time interval, will reflect these preferences. In order to study the sensitivity to changes in the forcing parameters S_k of (1) we have to identify a measure for the change in the behaviour of the T21QGL3 model. For a long term integration the amplitude a_1 of the projection onto EOF1 at level 500 hPa of each day, is calculated and then binned, thus creating the PDF₁ of a_1 . Each PDF _{i} is divided into 100 bins, each bin has the length 0.002. PDF₁ describes the intensity of the anomaly in the direction of EOF1. Only the level 500 hPa will be analysed. In Figure 3 PDFs of a_1 to a_6 for an unperturbed climate integration of 100,000 days are shown. The time mean of these PDFs vanishes, because (2b) implies

$$\overline{a_i(t)} = \overline{\langle \psi(t) - \overline{\psi(t)}, e^{(i)} \rangle} = \langle 0, e^{(i)} \rangle = 0,$$

where the overbar indicates the time mean. For a model integration with perturbed forcing parameters a same computation is made for the PDFs. Systematic changes in time of the EOF

amplitudes induce shifts in the PDFs indicating possible climatic change (changes in the frequency and duration of preferred patterns), see North et al. (1982) and Selten (1997). As a measure of change in the PDFs we introduce the parameter

$$\beta_i = \sum_{j=1}^{nbin} \{PDF_i(j) - PDF_i^{(0)}(j)\}^2, \quad (4)$$

where $PDF_i(j)$ is the probability of finding a_i in bin j for the system with the perturbed parameters; $PDF_i^{(0)}(j)$ is the one for the standard parameter values. It is of interest to find the largest changes from a small parameter vector perturbation of a given size. A larger β_i is expected to give a larger climate change. A PDF may just shift, or change its shape becoming wider or smaller or its skewness may change. In Cha and Srihari (2002) a large number of alternatives can be found for the measure (4) we have chosen. It is not expected that a different choice will substantially affect our results.

3. Directed search for effective forcing parameter perturbations

The forcing terms S_k in (1) are determined by computing the potential vorticity tendencies, using a large number of observed atmospheric fields and by averaging these tendencies (Roads, 1987). These average tendencies should be zero. This is equivalent to assuming that the sample of fields used in such a computation represents a statistically stable climatology. Consequently, the forcing term S_k must be chosen such that it compensates the deviation from zero:

$$S_k = J(\overline{\psi_k}, \overline{q_k}) - D_k(\overline{\psi}) + \overline{J(\psi'_k, q'_k)}, \quad (5)$$

where an apostrophe denotes the deviation from the averaged value. Corti et al. (1997) worked out this approach for the same model (1) using streamfunction fields from nine winter seasons.

Two questions can be raised: do small changes in the forcing parameters affect the simulated climate and is there an efficient way of finding the most effective forcing parameter perturbations? Standard methods, such as simulated annealing (Kirkpatrick et al, 1983), fail to give an answer within a reasonable computing time due to the long integration time of one run in combination with the large number of parameters that are varied. Since EOF1 is related to the most prominent preferred flow regime, it is very well possible that an additional constant forcing of the system in the direction of EOF1 turns out to be an effective way to change the climate. An alternative approach is found in the behaviour of circulation system near its (chaotic) attractor. At certain intervals trajectories near the attractor tend to diverge because of the fact that eigenvalues that correspond with the tangent linear system have a positive value. Then the system is likely to be more sensitive to perturbations. The idea is to choose a forcing perturbation in the direction of the eigenvector that corresponds with the largest eigenvalue of the tangent linear system integrated over a short time interval over which the linearization holds and the first eigenvalue takes a large positive value.

In order to come to a conclusion about the merits of these two approaches we also randomly select forcing perturbations in the next section. In each approach we integrate the full system over 100,000 days to verify the climate change induced by the perturbation and quantified by (4).

Perturbation in the direction of EOF1

As a first experiment, we add a forcing perturbation in the direction of EOF1, which is expected to change the amplitude of EOF1 of the streamfunction. A 100,000 day integration was made with

forcing parameter perturbed on each level individually with 5% of the climatological forcing in the direction of $e^{(1)}$:

$$\partial S_k = 0.05 \frac{|S|}{|e^{(1)}|} e_k^{(1)}, \quad k = 1, 2, 3, \quad (6)$$

so that indeed $|\partial S| = 0.05|S|$. It resulted in a PDF1 shift of $\beta_1 = 0.018$. Scaling the perturbation with 10%, gave a value of 0.050 for β_1 . In Figure 4 we show both shifts in the PDF.

Using a singular vector from the adjoint system along a reference orbit

Next we use an algorithm to calculate forcing singular vectors as devised by Barkmeijer et al, (2003). They compared singular vectors due to a change in initial conditions with those that arise from parametrical forcing in 2-day forecasts. Then the tangent linear and the corresponding adjoint model need to be extended with the equations with respect to the forcing parameters, which are coefficients of the parameter vector S . As mentioned in Section 2 it is assumed that the multi-level field of PV is a linear function of the multi-level streamfunction, which is invertible under appropriate boundary conditions. A time derivative of the streamfunction can be derived by eliminating the PV giving a system of the form

$$\frac{d\Psi}{dt} = F(\Psi; S), \quad (7)$$

where S denotes the forcing in terms of streamfunction. Next we consider the extended dynamical system with state vector

$$y = \begin{pmatrix} \Psi \\ S \end{pmatrix}.$$

The tendency equations then become:

$$\frac{dy}{dt} = \frac{d}{dt} \begin{pmatrix} \Psi \\ S \end{pmatrix} = \begin{pmatrix} F(\Psi, S) \\ 0 \end{pmatrix} = G(y). \quad (8)$$

The tangent linear equations are derived by linearizing Eq.(8) near a non-linear reference orbit y_r :

$$\frac{d(\delta y_r)}{dt} = J_G(y_r) \delta y_r \quad (9)$$

with Jacobi matrix

$$J_G(y_r) = \left[\frac{\partial G(y)}{\partial y} \right]_{y_r} = \begin{pmatrix} \partial F / \partial r & I \\ O & O \end{pmatrix}_{y_r},$$

where O is the zero matrix with the appropriate number of rows and columns. The presence of the identity matrix I is understood from the fact that the parameter vector only contains the constant forcing terms. The Jacobian matrix $\partial F / \partial r$ is obtained by linearizing Eq.(7) along a reference solution.

The tangent linear equations integrate a small perturbation $\delta y_r(0)$ forward in time over a sufficiently short period. This is described by the propagation matrix R :

$$\delta y_r(T) = R(0, T) \delta y_r(0). \quad (10)$$

At initial time the parameter perturbation is set fixed at the unit hypersphere $\langle \delta S(0), \delta S(0) \rangle = 1$ (due to the linearity of the system the size of the perturbation is irrelevant). The initial state $\psi(0)$ is not perturbed, so

$$\delta y_r(0) = \begin{pmatrix} 0 \\ \delta S(0) \end{pmatrix} = Q\delta S(0) \quad (11)$$

with Q an injective mapping. Substitution in (10) yields

$$\delta y_r(T) = R(0, T)Q\delta S(0). \quad (12)$$

Since we only have to consider the way $\delta\psi$ has evolved at time T , we use a surjective mapping P :

$$\delta\psi(T) = P\delta y_r(T) = PR(0, T)Q\delta S(0) = M\delta S(0). \quad (13)$$

In summary, integration of Eq.(8) maps vectors $\delta S(0)$ on a unit hypersphere in the forcing parameter space at the initial point ($t = 0$), to a set of vectors $\delta\psi(T)$ given by (13) forming an ellipsoid at the end point ($t = T$) in the state space of (7).

Our aim is to find the parameter perturbation δS , being constant in time, that causes the largest error growth at the end time. This is the vector δS that maximizes the ratio

$$\frac{\langle \delta\psi(T), N\delta\psi(T) \rangle^{1/2}}{\langle \delta S, N\delta S \rangle^{1/2}} = \frac{\langle M\delta S, NM\delta S \rangle^{1/2}}{\langle \delta S, N\delta S \rangle^{1/2}} = \frac{\langle M^*NM\delta S, \delta S \rangle^{1/2}}{\langle \delta S, N\delta S \rangle^{1/2}}, \quad (14)$$

where the matrix N specifies a norm based on the kinetic energy and the matrix M^* denotes the adjoint of M . Next we consider the following generalized eigenvalue problem

$$M^*NM\delta S = \lambda N\delta S \quad (15)$$

with largest eigenvalue λ having an eigenvector called the first singular vector. Using $v = N^{1/2}\delta S$ we rewrite (15) as an eigenvalue problem of a symmetric operator:

$$N^{-1/2}M^*NMN^{-1/2}v = \lambda v. \quad (16)$$

It is solved using the Lanczos algorithm (Parlett, 1980). The operator M is not explicitly known, it is evaluated by integrating the tangent linear equations. The operator M^* follows from a backward integration of the adjoint system (Barkmeijer et al., 2003). This procedure we apply over a short time interval of length T along the reference orbit with a perturbation δS of the forcing S giving the perturbation on the unit hypersphere that causes the largest change in $\delta\psi(T)$.

Selecting singular vectors in the peaks of the singular value as a function of time

It is expected that in time intervals with a large first eigenvalue (singular value) the system is sensitive to perturbations; particularly in the direction of the corresponding singular vector. Therefore, the search for the perturbation vector δS that results in the largest climate change is carried out as follows. With the use of the adjoint method forcing parameter perturbations that are likely to be effective are selected. The scheme is as follows:

- (a) Calculate a short reference orbit over a time interval of 5 days.

- (b) Calculate, with the use of the tangent linear and adjoint equations the corresponding first singular vector, along with the first singular value.
- (c) Shift the reference orbit a time step (one day) forward and calculate the corresponding first singular vector and the first singular value again.
- (d) Look at the evolution of the first singular value and select values that are local maxima above a threshold value of 500,000. Then use the corresponding first singular vector as forcing parameter perturbation.

The first singular value fluctuates considerably, as can be seen in Figure 5. Peaks mark the passage of a time interval in which the system is highly sensitive to parameter perturbations. Integrations of the full nonlinear system (7) are carried out over a length of 100,000 days with the 1000 largest first singular vectors as perturbations on the forcing parameters given by

$$\partial S_k = 0.05 \frac{|S|}{|v^{(1)}|} v_k^{(1)}, \quad k = 1, 2, 3, \quad (17)$$

where $v^{(1)}$ denotes a first singular vector that corresponds with one of the largest 1000 local maxima of the largest singular value. From each of these perturbed integrations PDF₁ of a_1 is calculated along with β_1 , see Figure 6 (dotted line). It falls very rapidly, but there is a long tail consisting of 8 runs with $\beta_1 > 0.020$. For the largest value of β_1 we found 0.037.

Selecting singular vectors just after the peaks of the singular value

In Moolenaar and Selten (2004) it is found that the singular vector that has just passed through a sensitive area is likely to be an effective parameter perturbation. Thus, we selected a singular value at the moment it has a first local minimum value after the peak. Again 1000 forcing perturbations are taken to compute PDF₁ and the shift of this PDF is computed. The largest value found for β_1 is now 0.050, which is more than a stroke of luck, because three times as much values are found

above $\beta_1 = 0.020$ than previously (at the peak of the first singular value itself). PDF_1 obtained from the singular vector as parameter perturbation direction that gave this largest β_1 is shown in Figure 7a. The distribution of all values of β_1 of the sample is given in Figure 6 (solid line).

4 Random selection of perturbations

In order to judge the value of our approach of selecting effective forcing parameter perturbations with the adjoint method, we compare our results with the best of 1000 randomly chosen perturbed forcing parameters. For each level, we draw randomly a vector from a set of uniformly distributed vectors on the unit hypersphere. Similar to (6) and (19) we perturb the climatic forcing S with 5% in the direction of the randomly chosen vector. Again integrations of 100,000 days are made, but this time with the randomly chosen parameter perturbations. The PDF of β_1 for these integrations is shown in Figure 6 (dashed line). The largest β_1 found with this random method equals 0.0025. This is a factor 20 smaller than the largest β_1 found with the second variant based on the adjoint method. From the vector perturbations found with this variant 35.7% yielded a larger β_1 than this largest value found with random selection. The shift in PDF_1 from the most effective random perturbation is shown in Figure 7b.

5. Conclusions

The goal of the method we presented is to find those parameter perturbations that cause the largest change in the climate statistics. For that purpose a GCM has to be integrated over a large time interval. Since for this problem a long computer time is required to evaluate the effect of a new set of parameter values, rigorous optimization methods cannot produce within a reasonable time span

the change of the parameter vector that results in the maximum climate change because of the large dimension of this parameter vector. As the first EOF can be related to a preferred weather regime, it is worth to study first the effect of a perturbation of the forcing parameter vector in the direction of this EOF. Next a method is presented that uses short time integrations of the adjoint equations at a reference orbit and selects perturbations that have a good chance to be effective in changing the climate. In a previous investigation (Moolenaar and Selten, 2004) the method was applied to the Lorenz 63 model. The encouraging results of that study made us decide to test the method for more realistic higher dimensional atmospheric circulation models. We took the T21QGL3 model.

To judge the outcome a comparison with a random selection method was made. In Table I we give the best result from a sample of 1000 parameter perturbations for each of the methods. It is noted that the adjoint method variant that picks the singular vector just after a peak in the largest singular value performs the best. From the tails of the PDFs of β_1 (Fig.6) it is seen that we are not dealing with a lucky guess for that method.

Although we do not exclude the possibility that in the future more efficient methods will be developed, we now have brought up a method that may create more openings in the field of uncertainty analysis of highly nonlinear systems. Moolenaar et al. (2007) carried out a sensitivity analysis for climate driven ecological systems with respect to the ecological parameters using the adjoint method. These parameters are also present in terms that are nonlinear in the state variables being comparable with terms in GCMs with products of state variables, being a situation that cannot be handled with uncertainty analysis methods based on a linearity assumption in case of small system perturbations. Although the adjoint equations become slightly more complex, the approach still continues to hold.

Acknowledgements

The authors thank J. Barkmeijer (KNMI) for allowing us to use his code to calculate the forcing singular vectors. They also thank J. Greenaway (ECMWF) for helping to run the model at the ECMWF computing facilities.

References

Allen, M.R., 2003: Possible or probable? *Nature*, **425**, 242.

Barkmeijer, J., T. Iversen and T.N. Palmer, 2003: Forcing singular vectors and other sensitive model perturbations. *Quart. J. Roy. Meteor. Soc.*, **129**, 2401-2424.

Carril A. F., S. Gualdi, A. Cherchi and A. Navarra, 2008 : Heatwaves in Europe: Areas of homogeneous variability and links with the regional to large-scale atmospheric and SSTs anomalies. *Climate Dyn.*, **30**, 77-98.

Cha, S-H., and S.N. Srihari, 2002: On measuring the distance between histograms, *Pattern Recognition*, **35**, 1355-1370.

Corti, S., A. Giannini, S. Tibaldi, and F. Molteni, 1997: Patterns of low-frequency variability in a three-level quasi-geostrophic model. *Climate Dyn.*, **13**, 883-904.

Errico, R.M., 1997: What is an adjoint model? *Bull. Amer. Meteor. Soc.*, **78**, 2577-2591.

Flemming, R.J., 1993: The dynamics of uncertainty: application to parametrization constants in climate models. *Climate Dyn.*, **8**, 135-150.

Gritsun, A., and G. Branstator, 2007: Climate response using a three-dimensional operator based on the fluctuation-dissipation theorem. *J. Atmos. Sci.*, **64**, 2558-2575.

Holton, J.R., 1992: *An Introduction to Dynamic Meteorology*. Third Edition, Academic Press.

Hurrell, J.W., 1995: Decadal trends in the North Atlantic Oscillation: Regional temperatures and precipitation. *Science*, **269**, 676-689.

IPCC, 2001. *Climate Change: The Scientific Basis*. Contribution of Working Group I, Third Assessment Report, Cambridge University Press.

Kirkpatrick, S., C.D. Gerlatt and M.P. Vecchi, 1983: Optimization by simulated annealing. *Science*, **220**, 671-680.

Leith, C.E., 1975: Climate response and fluctuation dissipation, *J. Atmos. Sci.*, **32**, 2022-2026.

Lorenz, E.N., 1956. Empirical orthogonal functions and statistical weather prediction. Scientific Report No.1, Department of Meteorology, MIT, 49pp.

Lorenz, E.N., 1963: Deterministic nonperiodic flow, *J. Atmos. Sci.*, **20**, 130-141.

Marshall, J., and F. Molteni, 1993: Towards a dynamical understanding of planetary-scale flow regimes. *J. Atmos. Sci.*, **50**, 1792-1818.

Molteni, F., and T.N. Palmer, 1993: Predictability and finite-time instability of the northern winter circulation. *Quart. J. Roy. Meteor. Soc.*, **19**, 269-298.

Moolenaar, H.E., and F.M. Selten, 2004: Finding the effective parameter perturbations in atmospheric models: the Lorenz63 model as case study. *Tellus*, **56A**, 47-55.

Moolenaar, H.E., J. Grasman, F.M. Selten and M. de Gee, M., 2007: Testing a method for analyzing the effect of parameter change in climate driven ecological systems. *Ecological Modelling*, **205**, 289-300.

Murphy, J.M., D.M.H. Sexton, D.N. Barnett, G.S. Jones, M.J. Webb, M. Collins and D.A. Stainforth, 2004: Quantification of modelling uncertainties in a large ensemble of climate change simulations. *Nature*, **430**, 768-772.

North, G.R., T.L. Bell, R.F. Cahalan and J.M. Moen, 1982: Sampling errors in the estimation of empirical orthogonal functions. *Mon. Wea. Rev.*, **110**, 699-706.

Oortwijn, J., and J. Barkmeijer, 1995: Perturbations that optimally trigger weather regimes. *J. Atmos. Sci.*, **52**, 3932-3944.

Parlett, B.N., 1980. *The Symmetric Eigenvalue Problem*. Prentice Hall.

Preisendorfer, R.W., 1988. *Principal Component Analysis in Meteorology and Oceanography*, Elsevier Science.

Roads, J.O., 1987: Predictability in the extended range. *J. Atmos. Sci.*, **44**, 3495-3527.

Selten, F.M., 1997: Baroclinic empirical orthogonal functions as basis in an atmospheric model. *J. Atmos. Sci.*, **54**, 2099-2114.

Selten, F.M., and G. Branstator, 2004: Preferred regime transition routes and evidence for an unstable periodic orbit in a baroclinic model. *J. Atmos. Sci.*, **61**, 2267-2282.

Stainforth, D.A., T. Aina, C. Christensen, M. Collins, N Faull, D.J. Frame, J.A. Kettleborough, S Knight, A Martin, J.M. Murphy, C. Piani, D. Sexton, L.A. Smith, R.A. Spicer, A.J. Thorpe and M.R. Allen, 2005: Uncertainty in predictions of the climate response to rising levels of greenhouse gases. *Nature*, **433**, 403-406.

Stocker, T.F., 2004: Models change their tunes, *Nature*, **430**, 737-738.

Visbeck, M., J.W. Hurrell, L. Polvani and H.M. Cullen, 2001: The North Atlantic Oscillation: Past, present, and future. *Proc. Nat. Acad. Sci.*, **98**, 12876-12877.

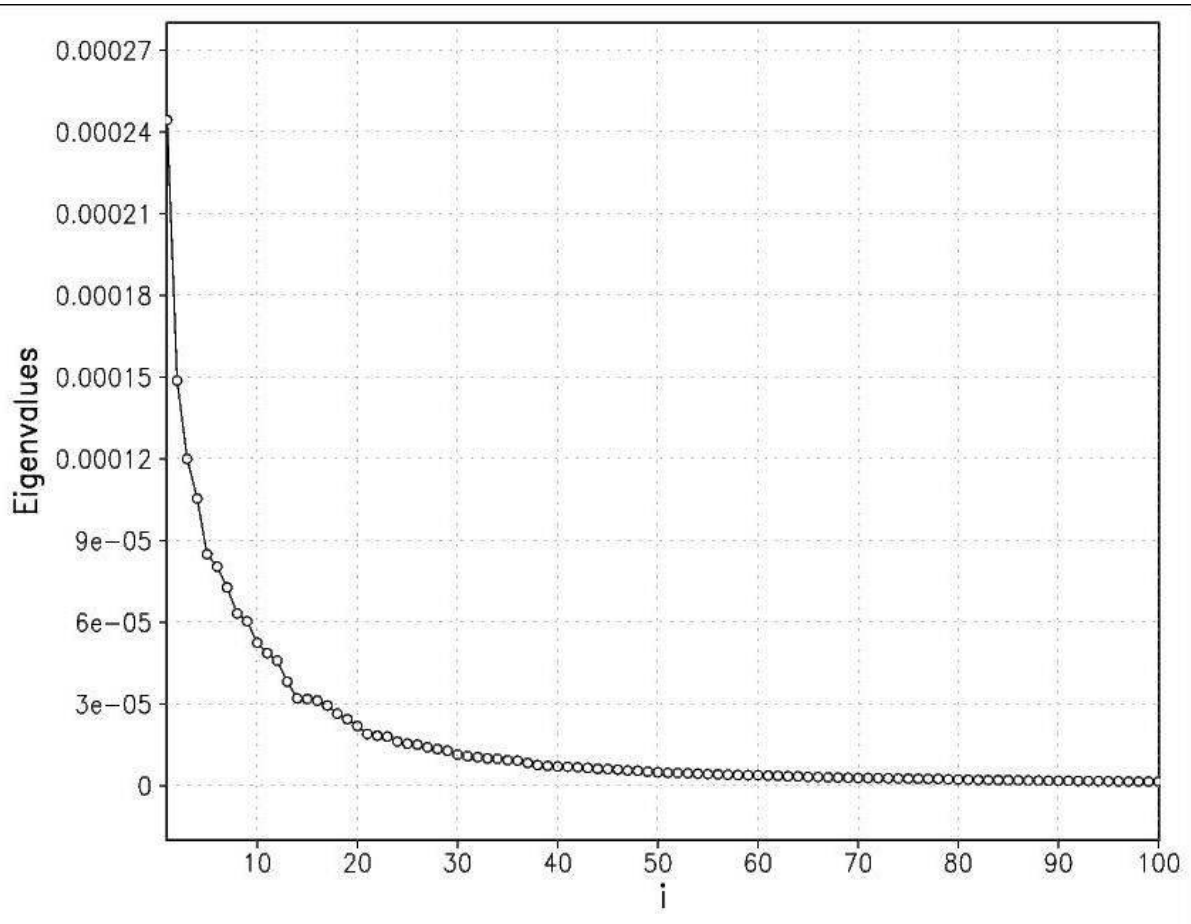


Figure 1: Eigenvalues μ_i of the matrix A , see (3). It is seen that most of the energy goes in the first EOFs.

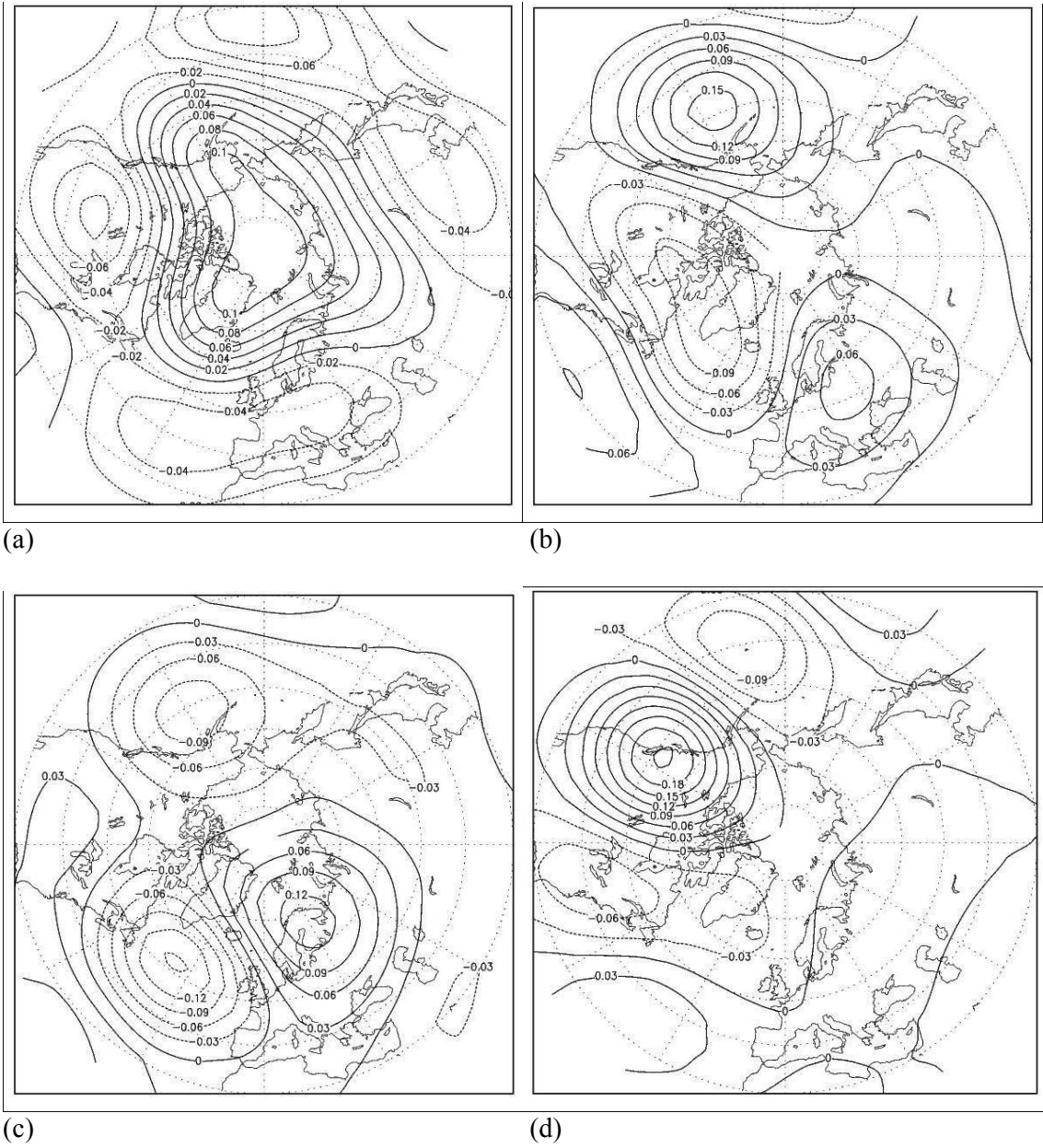


Figure 2: Preferred circulation patterns for the 500hPa streamfunction as indicated by the EOFs for the T21QGL3 model (a) EOF1, (b) EOF2, (c) EOF3 and (d) EOF4.

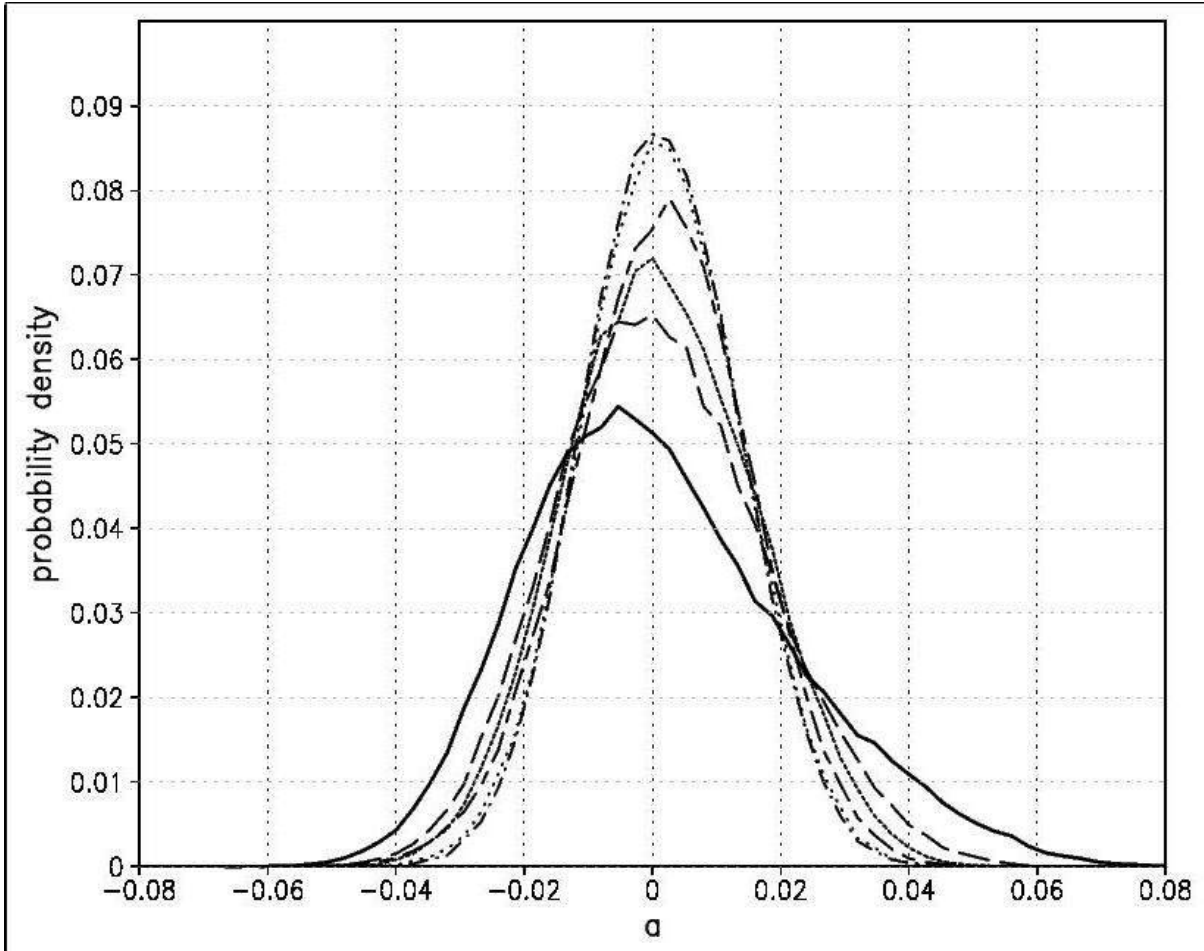


Figure 3: PDFs of the EOF amplitudes a_1 (solid), a_2 (long dash), a_3 (short dash), a_4 (long short dash), a_5 (dots), a_6 (dot dash). It is noted that the time means are all zero.

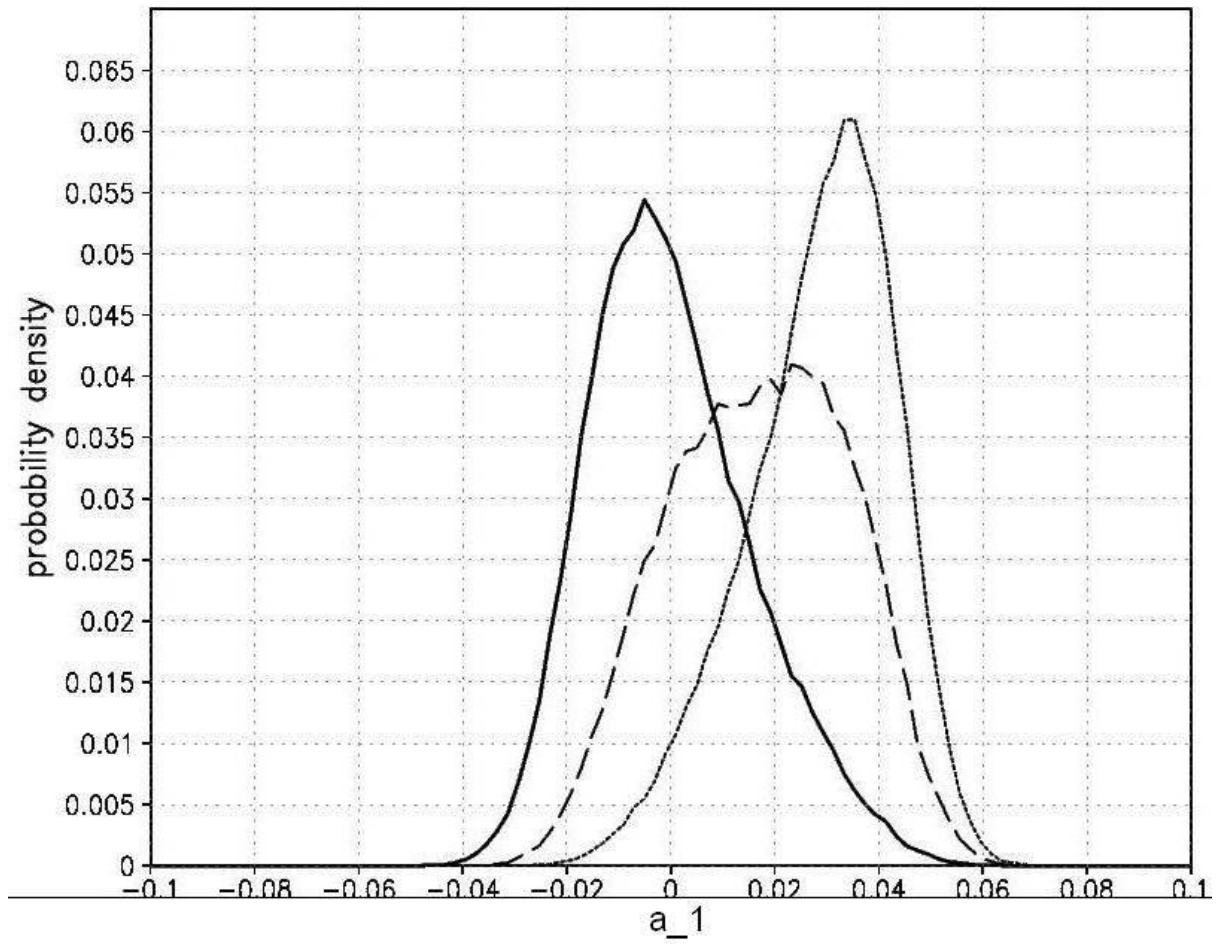


Figure 4: PDF1 of a_1 : (a) unperturbed (solid), (b) 5% perturbation in direction of EOF1 (dashed) with $\beta_1 = 0.018$, (c) 10% perturbation (dotted).

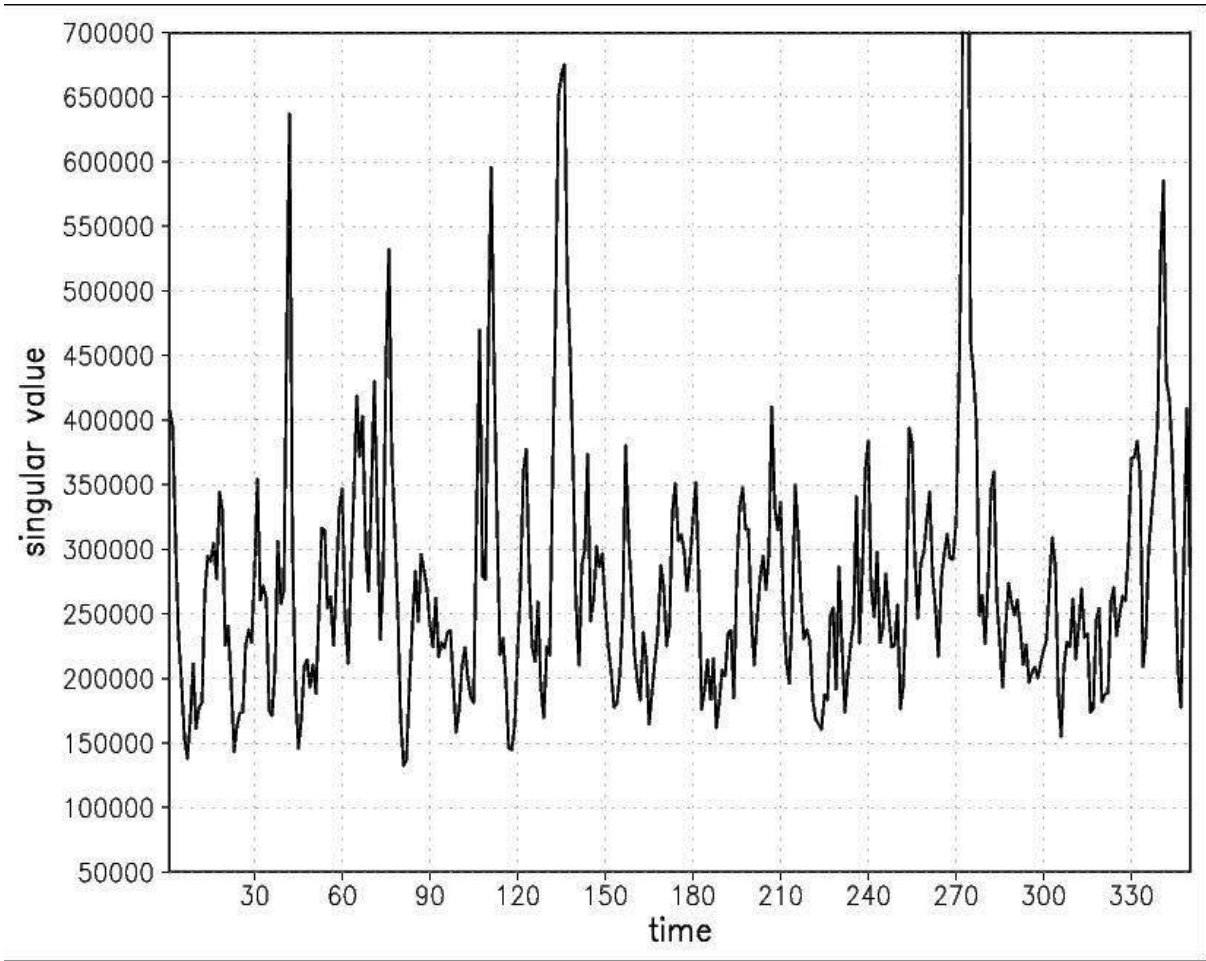


Figure 5: Evolution of the first singular value of (16) over 350 days for simulation runs over intervals of 5 days along a reference orbit with 4 days overlap of consecutive intervals.

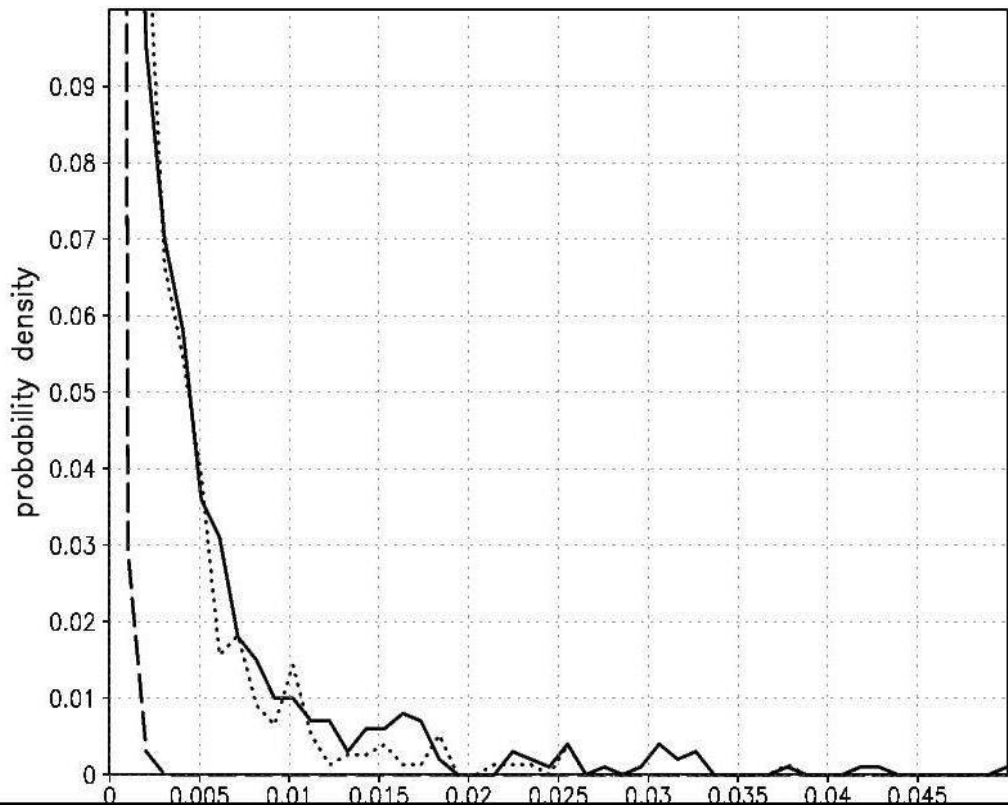


Figure 6: PDF of β_1 for a sample of 1000 runs by the adjoint method with direction of perturbation ∂S determined by (a) the singular vector at peaks of the first singular value (dotted), (b) the singular vector just after peaks of the first singular value (solid), (c) random selection (dashed).

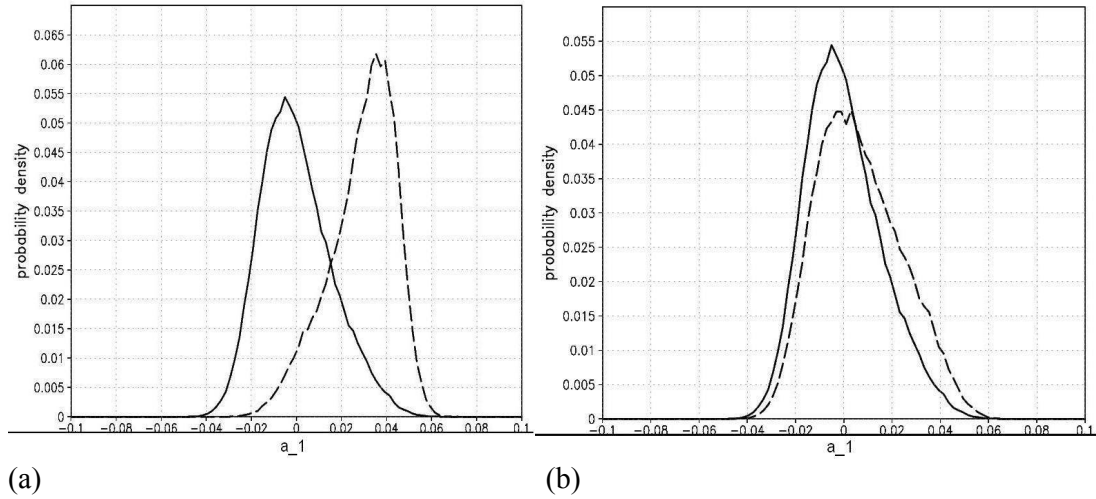


Figure 7: The solid line represents the PDF of a_1 for the unperturbed system: (a) the shifted PDF (dashed) due to a perturbation in the direction of the singular vector that corresponds with the first singular eigenvalue just after a peak producing the largest change in the PDF of a_1 : $\beta_1 = 0.05$, (b) the shifted PDF (dashed) due to the random perturbation of the sample that gives the largest change in a_1 : $\beta_1 = 0.0025$.

perturbation type (∂S)	max. PDF change (β_1)
in direction of EOF1	0.018
adjoint method (SV at peak)	0.037
adjoint method (SV just after peak)	0.050
random	0.0025

Table I Most effective perturbation direction of S from a selection of 1000 directions obtained with the different approaches.